



ELSEVIER

Contents lists available at ScienceDirect

International Journal of Mechanical Sciences

journal homepage: www.elsevier.com/locate/ijmecsci

A closed-form solution for natural frequencies of thin-walled cylinders with clamped edges



Marco Cammalleri*, Antonio Costanza

Department of Chemical, Management, Computer Science, Mechanical Engineering, University of Palermo, Viale delle Scienze, 90128 Palermo, Italy

ARTICLE INFO

Article history:

Received 27 November 2014

Received in revised form

26 November 2015

Accepted 5 March 2016

Available online 11 March 2016

Keywords:

Circular cylindrical shell

Natural frequencies

Free vibrations

Hamilton's principle

ABSTRACT

This paper presents an approximate closed-form solution for the free-vibration problem of thin-walled clamped–clamped cylinders. The used indefinite equations of motion are classic. They derive from Reissner's version of Love's theory, properly modified with Donnell's assumptions, but an innovative approach has been used to find the equations of natural frequencies, based on a solving technique similar to Rayleigh's method, on the Hamilton's principle and on a proper constructions of the eigenfunctions.

Thanks to the used approach, given the geometric and mechanical characteristics of the cylinder, the model provides the natural frequencies via a sequence of explicit algebraic equations; no complex numerical resolution, no iterative computation, no convergence analysis is needed.

The predictability of the model was checked both against FEM analysis results and versus experimental and numerical data of literature. These comparisons showed that the maximum error respect to the exact solutions is less than 10% for all the comparable mode shapes and less than 5%, on the safe side, respect to the experimental data for the lowest natural frequency.

There are no other models in the literature which are both accurate and easy to use. The accurate models require complex numerical techniques while the analytical models are not accurate enough. Therefore the advantage of this novel model respect to the others consists in a best balance between simplicity and accuracy; it is an ideal tool for engineers who design such shells structures.

© 2016 Elsevier Ltd. All rights reserved.

1. Introduction

Structural elements similar to thin-walled cylinders are widely used in several engineering fields; for example, cylindrical shell-like structures exist in pipelines, submarine hulls, aircraft fuselages and missiles. During mechanical processing needed for their manufacture or during their normal use, these elements are often stressed by time-varying forces; consequently, there is a need to characterize the vibratory behaviour to optimise the design and the production process.

The present paper is composed of five sections and an appendix. This section provides a short historical review of the numerical and analytical models of free vibrations of thin elastic shells. Section 2 presents the differential equations of motion. In Section 3 and in Appendix the mathematical basis of the present model is outlined, and the key equations are derived. A detailed analysis of the results, together with several comparisons with other models

and experimental data, is presented in Section 4, followed by conclusions in Section 5.

In the literature, there are several theories with various assumptions and simplifications about the vibrations of thin elastic shells; these theories typically are based on Love's indefinite equilibrium equations derived at the end of 19th century [1]. The research on this topic intensified during the 1960s and 1970s [2] and was further developed in the last two decades [3,4]. Over the years, linear models valid for small deformations were developed, along with non-linear models [5] also valid for large deformations.

In particular, the natural vibrations of thin-walled circular cylindrical shells were extensively analysed both from a theoretical point of view [6–13] and from an experimental point of view [6,7,11]; a recently published study aimed to adapt the classical theories to new applications based on carbon nanotubes [14]. However, due to the complexity of the problem, the exact solution of indefinite equations of motion only exists for circular cylindrical shells with two opposite shear diaphragm edges [12]. With other boundary conditions, the integration of these equations is generally performed with the aid of numerical methods; only in a few cases the solution has been found analytically, thanks to the introduction of special simplifying assumptions, but to the

* Corresponding author. Tel.: +39 091 23897256.

E-mail addresses: marco.cammalleri@unipa.it (M. Cammalleri), antonio.costanza@unipa.it (A. Costanza).

Nomenclature

a	mean radius of the cylinder [m]	\mathbf{x}	longitudinal unit vector [m]
A	amplitudes of the displacement functions [m]	x	longitudinal coordinate [m]
D	bending rigidity of the thin wall [N m]	X	dimensionless longitudinal coordinate
E	Young's modulus [N m ⁻²]	α	model dimensionless parameter (see Eq. (26))
f	natural frequency [Hz]	β	rotations of the tangents to the reference surface [rad]
\mathbf{F}	resultant force vectors per unit length [N m ⁻¹]	γ	shear deformation of the reference surface
G	shear modulus [N m ⁻²]	$\gamma(\zeta)$	shear deformation of a generic point
H	Hamiltonian action [J s]	Δ	dimensionless frequency factor
h	wall thickness of the cylinder [m]	ε	normal deformations of the reference surface
k	curvatures of the reference surface [m ⁻¹]	$\varepsilon(\zeta)$	normal deformations of a generic point
K	extensional rigidity of the shell wall [N m ⁻¹]	ζ	radial distance of a generic point from the reference surface [m]
l	length of the cylinder [m]	η_1, η_2	model dimensionless parameter (see Eqs. (21) and (22))
L	Lagrangian function [J]	θ	dimensionless circumferential coordinate [rad]
m	number of longitudinal half-waves	μ	model dimensionless parameter (see Eqs. (14) and (17))
\mathbf{M}	resultant moment vectors per unit length [N]	ν	Poisson's ratio
M	moments, per unit length, acting on the infinitesimal element [N]	ξ	model dimensionless parameter (see Eq. (20))
n	number of circumferential waves	ρ	material density [kg m ⁻³]
N	forces, per unit length, acting on the infinitesimal element [N m ⁻¹]	τ	torsion of the reference surface [rad m ⁻¹]
Q	transverse shear forces, per unit length, acting on the infinitesimal element [N m ⁻¹]	φ	model dimensionless parameter (see Eq. (26))
\mathbf{r}	radial unit vector [m]	Ψ	model dimensionless parameter (see Eq. (12))
r	radial coordinate [m]	ω	circular frequency [rad s ⁻¹]
R_1, R_2, R_3	coefficients of the frequency equation		
\mathbf{s}	circumferential unit vector [m]	<i>Subscripts</i>	
s	circumferential coordinate [m]	s	circumferential direction
t	time [s]	r	radial direction
u	displacements of the reference surface [m]	x	longitudinal direction
W	virtual work [J]		

detriment of accuracy or applicability domain. Arnold and Warburton [6] were among the first to study this type of problem; using the energy method and Timoshenko's relationships [15], they obtained a closed-form approximation of the natural frequencies for the case of simply supported edges. Koval and Cranch [7] studied the case of clamped-clamped edges using Donnell's equations [16] and provide an analytical solution as in this paper, but their model gets a limited applicability domain due to several oversimplifications. The same issue was addressed by Smith and Haft [8] using Flügge's equations [17] decoupled by Yu [18] but in this case as well, the problem was only solved numerically. Also Xuebin [19] used the Flügge's equations but introducing a new form of variables separation for arbitrary boundary conditions and applying the Newton-Raphson iteration method for the resolution of the frequency equation. Chung [20], using the Sanders' shell equations, obtained the expression of the frequency equation for any kind of boundary condition, but with the aid of iterative numerical method. Callahan and Baruh [9] obtained the natural frequencies analytically for several boundary conditions using Junger and Feit's equations [21]. However, the calculation was based on coefficients dependent on the constraints of geometry and material characteristics, which can be determined only numerically; therefore, this is not really a closed-form model. Wang and Lai [10] introduced a novel approach based on the wave theory and on the well-known Love's equations, which allowed them a closed-form resolution for different boundary conditions, clamped-clamped included as in this paper; however, the solution results inaccurate for the simpler mode shapes, as occurred for the Koval and Cranch [7] model. Pellicano [11] conducted both theoretical and experimental analyses on linear and nonlinear

vibration based on the Sanders-Koiter theory [22–23] for different boundary conditions; in this case, the analysis was also performed using numerical resolution techniques. Recently, further approaches to the problem were developed: Xing et al. [12], working from the Donnell-Mushtari theory [24], resolved the problem for different boundary conditions via the variables separation method associated with the Newton iterative method; moreover, both Xie et al. [13] and Zhang et al. [25] analysed different boundary conditions using the Goldenveizer-Novozhilov theory [26] but with different numerical approaches, the former used the Haar wavelet numerical method, while the latter used the local adaptive differential quadrature method. Khalili et al. [27] presented a formulation of 3D refined higher-order shear deformation theory for the free vibration analysis of simply supported-simply supported and clamped-clamped cylindrical shells and the solutions are obtained using the Galerkin numerical method.

The literature review found no models for the free-vibration problem of clamped-clamped cylinders, which are both accurate and easy to use. The accurate models require complex numerical techniques while the analytical models are not accurate enough. The novel model presented here, in contrast, combines good accuracy with ease and speed of calculation: it carefully provides the natural frequencies via a simple sequence of explicit algebraic equations; no complex numerical resolution, no iterative computation, no convergence analysis is needed, unlike other models in the literature or FEM analysis.

The used indefinite motion equations were classic, but an innovative approach was used to find the equations of natural frequencies based on a solving technique similar to Rayleigh's

method, on the Hamilton's principle and on a proper constructions of the eigenfuctions.

The predictability of the model was checked both against FEM modal analysis and versus experimental and numerical data of literature. These comparisons showed that maximum error respect to the exact solutions is less than 10% for all the comparable mode shapes and less than 5%, on the safe side, respect to the experimental data for the lowest natural frequency.

The advantage of this novel model respect to the others consists in a best balance between simplicity and accuracy; therefore it is an ideal tool for engineers who design such shells structures.

2. Differential equations of motion

The indefinite equations of motion used in this paper derive from Reissner's version [28] of Love's theory [1] modified with Donnell's assumptions [16], without the introduction of further simplifications.

Consider a thin-walled circular cylindrical shell, of finite length l , constant thickness h and mean radius a (see Fig. 1) consisting of material having a density ρ , Young's modulus E and Poisson's ratio ν . Fig. 1 shows the reference surface corresponding to the mean radius and the orthogonal local reference system consisting of longitudinal direction x , circumferential direction s and radial direction r .

Fig. 2 shows the graphical representation of the forces and moments that arise from the internal stress state and act on the infinitesimal element of the shell. Such internal actions, as well as the inertial forces, are defined per unit of arc length on the reference surface and are considered applied on it.

The forces N_x , Q_x and N_{xs} acting on the x =constant face are the components of the vector \mathbf{F}_x , whereas the forces N_s , Q_s and N_{sx} acting on the s =constant face are the components of the vector \mathbf{F}_s :

$$\mathbf{F}_x = N_x \mathbf{x} + N_{xs} \mathbf{s} - Q_x \mathbf{r}, \quad \mathbf{F}_s = N_{sx} \mathbf{x} + N_s \mathbf{s} - Q_s \mathbf{r},$$

where \mathbf{x} , \mathbf{s} and \mathbf{r} represent the triad of unit vectors of the local reference system. Similarly, the moments M_x and M_{xs} acting on the

x =constant face are the components of the vector \mathbf{M}_x , while the moments M_s and M_{sx} acting on the s =constant face are the components of the vector \mathbf{M}_s :

$$\mathbf{M}_x = -M_{xs} \mathbf{x} + M_x \mathbf{s}, \quad \mathbf{M}_s = -M_s \mathbf{x} + M_{sx} \mathbf{s}.$$

The indefinite equations of motion for a thin-walled circular cylindrical shell can be written as follows [28]:

$$\begin{aligned} \frac{\partial N_x}{\partial x} + \frac{\partial N_{sx}}{\partial s} &= \rho h \frac{\partial^2 u_x}{\partial t^2}, \\ \frac{\partial N_{xs}}{\partial x} + \frac{\partial N_s}{\partial s} + \frac{Q_s}{a} &= \rho h \frac{\partial^2 u_s}{\partial t^2}, \\ \frac{\partial Q_x}{\partial x} + \frac{\partial Q_s}{\partial s} - \frac{N_s}{a} &= \rho h \frac{\partial^2 u_r}{\partial t^2}, \end{aligned} \tag{1}$$

$$\frac{\partial M_x}{\partial x} + \frac{\partial M_{sx}}{\partial s} - Q_x = 0,$$

$$\frac{\partial M_{xs}}{\partial x} + \frac{\partial M_s}{\partial s} - Q_s = 0$$

The displacements u_x , u_s , u_r and the rotations β_x , β_s of the tangents along x and s (showed in Fig. 3), the deformations ϵ_x , ϵ_s , γ_{xs} , the curvatures k_x , k_s and the torsion τ are related by the following congruence equations [28]:

$$\epsilon_x = \frac{\partial u_x}{\partial x}, \quad \epsilon_s = \frac{\partial u_s}{\partial s} + \frac{u_r}{a}, \quad \gamma_{xs} = \frac{\partial u_s}{\partial x} + \frac{\partial u_x}{\partial s} \tag{2.1}$$

$$\beta_x = -\frac{\partial u_r}{\partial x}, \quad \beta_s = \frac{u_s}{a} - \frac{\partial u_r}{\partial s} \tag{2.2}$$

$$\begin{aligned} k_x &= \frac{\partial \beta_x}{\partial x} = -\frac{\partial^2 u_r}{\partial x^2}, \quad k_s = \frac{\partial \beta_s}{\partial s} = \frac{\partial}{\partial s} \left(\frac{u_s}{a} - \frac{\partial u_r}{\partial s} \right), \\ \tau &= \frac{\partial \beta_s}{\partial x} + \frac{\partial \beta_x}{\partial s} = \frac{1}{a} \frac{\partial u_s}{\partial x} - 2 \frac{\partial^2 u_r}{\partial x \partial s} \end{aligned} \tag{2.3}$$

where all quantities relate to the reference surface.

The deformations of a generic point distant ζ from the reference surface can be written as follows:

$$\epsilon_x(\zeta) = \epsilon_x + \zeta k_x, \quad \epsilon_s(\zeta) = \epsilon_s + \zeta k_s, \quad \gamma_{xs}(\zeta) = \gamma_{xs} + \zeta \tau \tag{3}$$

where the second terms represent the bending contributions to the deformation.

Part of the formulation described above may be simplified by using the approximations first advanced by Donnell [16]. The first assumption concerns the indefinite equations of motion and considers the term Q_s/a negligible in the equilibrium of the forces along the circumferential direction s ; Eq. (1) are thus reduced to the following system:

$$\begin{aligned} \frac{\partial N_x}{\partial x} + \frac{\partial N_{sx}}{\partial s} &= \rho h \frac{\partial^2 u_x}{\partial t^2}, \\ \frac{\partial N_{xs}}{\partial x} + \frac{\partial N_s}{\partial s} &= \rho h \frac{\partial^2 u_s}{\partial t^2}, \end{aligned} \tag{4}$$

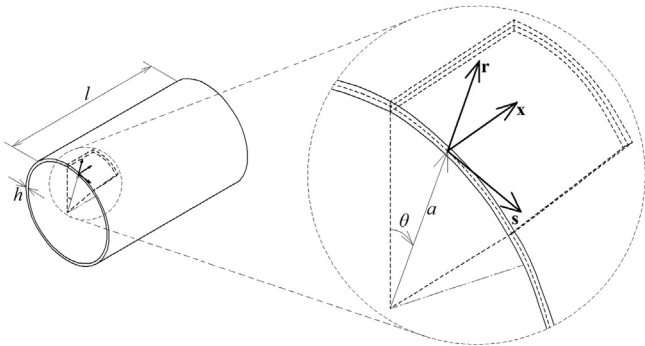


Fig. 1. Geometry, middle reference surface and local reference system (x , s , r) of a thin cylindrical shell.

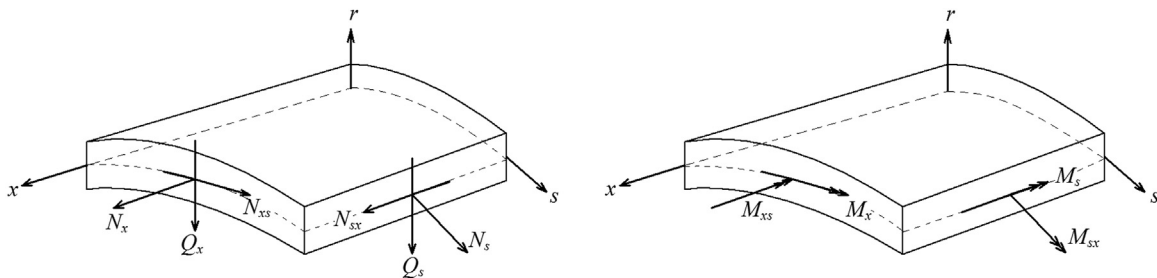


Fig. 2. Internal forces and moments acting on the infinitesimal element of the shell.

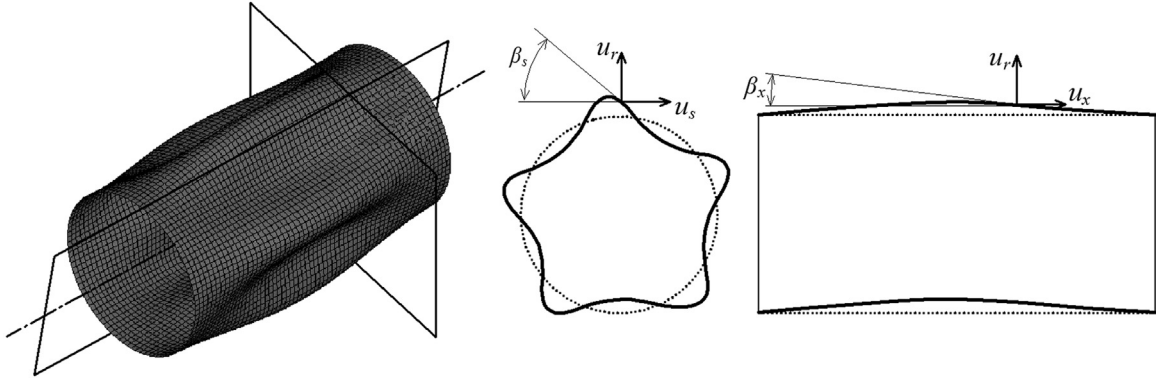


Fig. 3. Displacements and rotations in a generic point of a clamped-clamped cylinder. (a) Deformed cylinder (b) Cross section (c) Longitudinal section.

$$\frac{\partial^2 M_x}{\partial x^2} + 2 \frac{\partial^2 M_{xs}}{\partial x \partial s} + \frac{\partial^2 M_s}{\partial s^2} - \frac{N_s}{a} = \rho h \frac{\partial^2 u_r}{\partial t^2}$$

where the third equation was obtained by combining the last equations of (1). The second assumption concerns the congruence Eq. (2.3); it is assumed that variation in the circumferential displacement u_s does not influence the curvature k_s and the torsion τ ; Eq. (2.3) are then reduced to:

$$k_x = -\frac{\partial^2 u_r}{\partial x^2}, \quad k_s = -\frac{\partial^2 u_r}{\partial s^2}, \quad \tau = -2 \frac{\partial^2 u_r}{\partial x \partial s} \quad (5)$$

These latter Eq. (5) are equal to the corresponding equations of the plate theory [15]. The two assumptions explained above are equivalent to stating that a thin walled cylinder with relatively small curvature behaves similarly to a thin plate; the only differences, due to the curvature of the wall, are the presence of N_s/a in the third equation of motion and the presence of u_r/a in the equation for normal deformation in the circumferential direction ϵ_s . Finally, the constitutive equations are as follows [28]:

$$\begin{aligned} N_x &= K(\epsilon_x + \nu \epsilon_s), \quad N_s = K(\epsilon_s + \nu \epsilon_x), \\ N_{xs} &= N_{sx} = \frac{K(1-\nu)}{2} \gamma_{xs} = Gh \gamma_{xs}, \\ M_x &= D(k_x + \nu k_s), \quad M_s = D(k_s + \nu k_x), \\ M_{xs} &= M_{sx} = \frac{D(1-\nu)\tau}{2} = Gh^3 \tau / 12 \end{aligned} \quad (6)$$

where G is the shear modulus and

$$K = \frac{Eh}{1-\nu^2}, \quad D = \frac{Eh^3}{12(1-\nu^2)}$$

are, respectively, the extensional and bending rigidity of the shell wall.

Substituting the congruence Eqs. (2.1), (2.2) and (5) into the constitutive Eq. (6) and subsequently replacing into the indefinite equations of motion (4), the latter are expressed as functions of the displacements:

$$\begin{aligned} K \left(\frac{\partial^2 u_x}{\partial x^2} + \frac{1-\nu}{2a^2} \frac{\partial^2 u_x}{\partial \theta^2} + \frac{1+\nu}{2a} \frac{\partial^2 u_s}{\partial x \partial \theta} + \frac{\nu}{a} \frac{\partial u_r}{\partial x} \right) &= \rho h \frac{\partial^2 u_x}{\partial t^2}, \\ K \left(\frac{1+\nu}{2a} \frac{\partial^2 u_x}{\partial x \partial \theta} + \frac{1-\nu}{2} \frac{\partial^2 u_s}{\partial x^2} + \frac{1}{a^2} \frac{\partial^2 u_s}{\partial \theta^2} + \frac{1}{a^2} \frac{\partial u_r}{\partial \theta} \right) &= \rho h \frac{\partial^2 u_s}{\partial t^2}, \end{aligned} \quad (7)$$

$$K \left[-\frac{\nu}{a} \frac{\partial u_x}{\partial x} - \frac{1}{a^2} \frac{\partial u_s}{\partial \theta} - \frac{u_r}{a^2} - \frac{h^2}{12} \left(\frac{\partial^4 u_r}{\partial x^4} + \frac{1}{a^4} \frac{\partial^4 u_r}{\partial \theta^4} + \frac{2}{a^2} \frac{\partial^4 u_r}{\partial x^2 \partial \theta^2} \right) \right] = \rho h \frac{\partial^2 u_r}{\partial t^2}$$

where $\theta = s/a$.

Finally, the clamped-clamped boundary conditions require that both the displacements and the rotations vanish at either edges (see Fig. 3a), and then are expressed by the following equations:

$$\begin{cases} u_x = u_s = u_r = 0 \\ \beta_x = \beta_s = 0 \end{cases} \quad \text{for } x = 0 \text{ and } x = l \quad (8)$$

3. Equation of natural frequencies

A procedure similar to Rayleigh's method was used to determine the natural frequencies of the system. Based on the considerations presented below, three displacement functions u_x , u_s , u_r , were defined and adopted as the eigenfunctions of the problem. However, the corresponding eigenvalues were identified by making Hamilton's action constant instead of making Rayleigh's quotient constant. In fact, Hamilton's principle declares that the natural motions of a mechanical system in which the extreme configurations are known are those that make the Hamiltonian action H constant for each possible configuration. For a conservative system, this principle mathematically becomes:

$$\delta H = \delta \int_{t_0}^{t_1} L dt = 0 \quad (9.1)$$

or

$$\int_{t_0}^{t_1} \delta W dt = 0 \quad (9.2)$$

where L is the Lagrangian function (difference between the kinetic and potential energy of the system), t_0 and t_1 are the generic temporal limits of integration and δW is the virtual work performed by all forces present in the system, including the inertial forces.

The second formulation (9.2) allows one to write Hamilton's principle without deriving the Lagrangian function L when the equations of motion are already known. In this case, the virtual work δW can be easily expressed by multiplying each of the undefined scalar equations of motion for a virtual reversible displacement along the corresponding direction and so, using Eq. (7):

$$\delta W = aK \int_0^{2\pi} \int_0^l \left\{ \begin{aligned} &\left[\frac{\partial^2 u_x}{\partial x^2} + \frac{1-\nu}{2a^2} \frac{\partial^2 u_x}{\partial \theta^2} + \frac{1+\nu}{2a} \frac{\partial^2 u_s}{\partial x \partial \theta} + \frac{\nu}{a} \frac{\partial u_r}{\partial x} - \frac{1-\nu^2}{E} \rho \frac{\partial^2 u_x}{\partial t^2} \right] \delta u_x + \left[\frac{1+\nu}{2a} \frac{\partial^2 u_x}{\partial x \partial \theta} + \frac{1-\nu}{2} \frac{\partial^2 u_s}{\partial x^2} + \frac{1}{a^2} \frac{\partial^2 u_s}{\partial \theta^2} + \frac{1}{a^2} \frac{\partial u_r}{\partial \theta} - \frac{1-\nu^2}{E} \rho \frac{\partial^2 u_s}{\partial t^2} \right] \delta u_s \\ &- \left[\frac{\nu}{a} \frac{\partial u_x}{\partial x} + \frac{1}{a^2} \frac{\partial u_s}{\partial \theta} + \frac{u_r}{a^2} + \frac{h^2}{12} \left(\frac{\partial^4 u_r}{\partial x^4} + \frac{1}{a^4} \frac{\partial^4 u_r}{\partial \theta^4} + \frac{2}{a^2} \frac{\partial^4 u_r}{\partial x^2 \partial \theta^2} \right) + \frac{1-\nu^2}{E} \rho \frac{\partial^2 u_r}{\partial t^2} \right] \delta u_r \end{aligned} \right\} dx d\theta \quad (10)$$

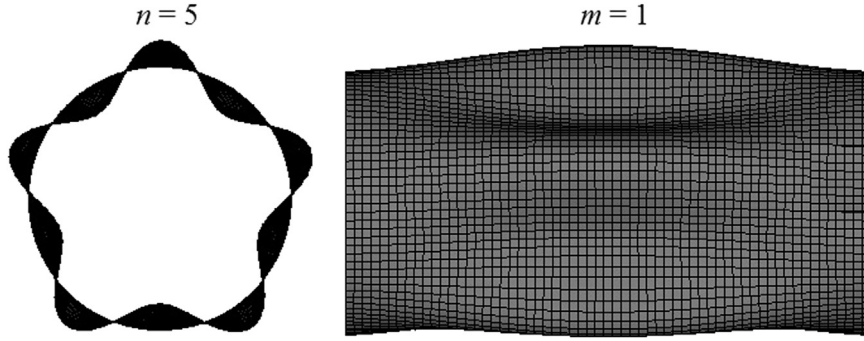


Fig. 4. Mode shape of a thin-walled circular cylinder with clamped edges; $n=5$ and $m=1$ (image resulting from FEM modal analysis).

The deformation in free vibration of a thin-walled circular cylinder consists of a positive integer n of waves on the section orthogonal to the axis and a positive integer m of half-waves on the section containing the axis, henceforth called circumferential waves and longitudinal half-waves, respectively. Therefore, each mode shape is characterized by a pair of values of n and m (see, for example, Fig. 4).

The shape of the circumferential waves is independent of the boundary conditions, while the shape of the longitudinal half-waves depends on boundary conditions and is similar to the flexural vibrations of beams subject to the same constraints [10,13].

These considerations, together with the need to construct eigenfunctions that, respecting the constraint conditions and mutual orthogonality, were analytically manageable in the subsequent steps of derivation and integration, led the authors to distinguish between odd and even numbers of longitudinal half-waves (see Appendix for more details). For odd m :

$$u_x = A_x \left[-\sin \mu \left(\frac{1}{2} - X \right) + \Psi \sinh \mu \left(\frac{1}{2} - X \right) \right] \cos n\theta \cos \omega t,$$

$$u_s = A_s \left[\cos \mu \left(\frac{1}{2} - X \right) + \Psi \cosh \mu \left(\frac{1}{2} - X \right) \right] \sin n\theta \cos \omega t, \quad (11)$$

$$u_r = A_r \left[\cos \mu \left(\frac{1}{2} - X \right) + \Psi \cosh \mu \left(\frac{1}{2} - X \right) \right] \cos n\theta \cos \omega t,$$

where A_x , A_s and A_r are arbitrary coefficients, ω is the circular frequency, $X=x/l$ and, to comply with the boundary conditions,

$$\Psi = \frac{\sin(\mu/2)}{\sinh(\mu/2)}. \quad (12)$$

The quantity μ must satisfy the equation

$$\tan \frac{\mu}{2} + \tanh \frac{\mu}{2} = 0, \quad (13)$$

whose roots are (in addition to the value 0):

$$\mu \approx [1.506 + (m-1)\pi], \quad (14)$$

for $m=1, 3, 5, 7$

For even m , the eigenfunctions become:

$$u_x = A_x \left[-\cos \mu \left(\frac{1}{2} - X \right) + \Psi \cosh \mu \left(\frac{1}{2} - X \right) \right] \cos n\theta \cos \omega t,$$

$$u_s = A_s \left[\sin \mu \left(\frac{1}{2} - X \right) - \Psi \sinh \mu \left(\frac{1}{2} - X \right) \right] \sin n\theta \cos \omega t \quad (15)$$

$$u_r = A_r \left[\sin \mu \left(\frac{1}{2} - X \right) - \Psi \sinh \mu \left(\frac{1}{2} - X \right) \right] \cos n\theta \cos \omega t,$$

in which the quantity μ satisfies the equation

$$\tan \frac{\mu}{2} - \tanh \frac{\mu}{2} = 0, \quad (16)$$

whose roots are (in addition to the value 0):

$$\mu \approx [2.500 + (m-2)\pi], \quad (17)$$

for $m=2, 4, 6, 8, \dots$

and Ψ is again Eq. (12).

Substituting into Eq. (10) both the partial derivatives $\partial \dots$ and the virtual displacements $\delta \dots$ of u_x , u_s and u_r , and integrating with respect to x and θ gives the elementary virtual work. Subsequently, integrating Eq. (9.2) with respect to time t , after intricate manipulation, gives:

$$\left\{ \left[\xi^2 \eta_1 + \frac{1}{2}(1-\nu)n^2 \eta_2 - \eta_2 \Delta \right] A_x - \frac{1}{2}(1+\nu)\xi n \eta_2 A_s - \xi \nu \eta_2 A_r \right\} \delta A_x + \left\{ -\frac{1}{2}(1+\nu)\xi n \eta_2 A_x + \left[n^2 \eta_1 + \frac{1-\nu}{2} \xi^2 \eta_2 - \eta_1 \Delta \right] A_s + n \eta_1 A_r \right\} \delta A_s + \left\{ \xi \nu \eta_2 A_x - n \eta_1 A_s - \left[\eta_1 - \eta_1 \Delta + \frac{h^2}{12a^2} (\xi^4 \eta_1 + n^4 \eta_1 + 2\xi^2 n^2 \eta_2) \right] A_r \right\} \delta A_r = 0 \quad (18)$$

where

$$\Delta = \rho a^2 (1-\nu^2) \frac{\omega^2}{E} \quad (19)$$

is the dimensionless frequency factor and

$$\xi = \frac{\mu a}{l} \quad (20)$$

Moreover, for an odd number m of longitudinal half-waves

$$\eta_1 = 1 + \Psi^2, \quad \eta_2 = 1 - \Psi^2 + \frac{2}{\mu} \sin \mu, \quad (21)$$

while for an even number m of longitudinal half-waves,

$$\eta_1 = -1 + \Psi^2, \quad \eta_2 = -1 - \Psi^2 + \frac{2}{\mu} \sin \mu. \quad (22)$$

Because the quantities δA_x , δA_s and δA_r are arbitrary, Eq. (18) can be satisfied only if the quantities in the braces vanish individually. If these quantities are set to zero, a homogeneous system of three linear equations in three unknowns is obtained: A_x , A_s and A_r . To avoid the trivial solution, the determinant of the coefficients is set to zero, giving the following cubic equation for the frequency factor Δ :

$$\Delta^3 - R_2 \Delta^2 + R_1 \Delta - R_0 = 0, \quad (23)$$

where

$$R_2 = \left(\frac{\eta_1}{\eta_2} + \frac{1-\nu}{2} \frac{\eta_2}{\eta_1} \right) \xi^2 + 1 + \frac{3-2\nu}{2} n^2 + \frac{h^2}{12a^2} \left(\xi^4 + n^4 + 2\xi^2 n^2 \frac{\eta_2}{\eta_1} \right), \\ R_1 = \frac{1-\nu}{2} \left(\xi^4 + n^4 \right) + \left(\frac{\eta_1 - \nu \eta_2}{\eta_2} \right) \xi^2 n^2 + \frac{1-\nu}{2} n^2 + \xi^2 \left[\frac{\eta_1 + \eta_2}{\eta_2} + \frac{\eta_2 (1-\nu-2\nu^2)}{\eta_1} \right] \\ + \frac{h^2}{12a^2} \left[\frac{1-\nu}{2} \left(n^2 + \xi^2 \frac{\eta_2}{\eta_1} \right) + n^2 + \xi^2 \frac{\eta_1}{\eta_2} \right] \left(\xi^4 + n^4 + 2\xi^2 n^2 \frac{\eta_2}{\eta_1} \right) \quad (24)$$

$$R_0 = \frac{1-\nu}{2} \left[1 - \nu \left(\frac{\eta_2}{\eta_1} \right)^2 \right] \xi^4 + \frac{h^2}{12a^2} \left\{ \xi^2 n^2 \left[\frac{1+\nu}{2} \frac{\eta_2}{\eta_1} - \frac{\eta_1}{\eta_2} - \left(\frac{1-\nu}{2} \right)^2 \frac{\eta_2}{\eta_1} \right] + \frac{1-\nu}{2} (\xi^4 + n^4) \right\} \left(\xi^4 + n^4 + 2\xi^2 n^2 \frac{\eta_2}{\eta_1} \right).$$

Eq. (23) has three different, real and positive roots:

$$\begin{aligned} \Delta_1 &= 2\alpha^{1/3} \cos \frac{\varphi + 2\pi}{3} + \frac{R_2}{3}, \\ \Delta_2 &= 2\alpha^{1/3} \cos \frac{\varphi + 4\pi}{3} + \frac{R_2}{3}, \\ \Delta_3 &= 2\alpha^{1/3} \cos \frac{\varphi}{3} + \frac{R_2}{3}, \end{aligned} \tag{25}$$

where

$$\alpha = \left[-\frac{1}{27} \left(R_1 - \frac{R_2^2}{3} \right)^3 \right]^{1/2}, \quad \varphi = \arccos \left[\frac{1}{2\alpha} \left(R_0 - \frac{R_1 R_2}{3} + \frac{2R_2^3}{27} \right) \right]. \tag{26}$$

Once the values of Δ_1 , Δ_2 and Δ_3 were known, the three natural frequencies f_1 , f_2 and f_3 were calculated by simple manipulation of Eq. (19):

$$f_{1,2,3} = \frac{\omega_{1,2,3}}{2\pi} = \frac{1}{2\pi a} \sqrt{\frac{E \Delta_{1,2,3}}{\rho(1-\nu^2)}}. \tag{27}$$

Despite the complex mathematics used to obtain the natural frequencies (27), the practical use of the model is much simpler; given the geometric and mechanical characteristics of the cylinder (length l , mean radius a , thickness h , Young's modulus E , Poisson's ratio ν and density ρ), for fixed mode shape (values m and n) the following parameters are sequentially calculated using algebraic equations: μ via (14) or (17), ψ and ξ via (12) and (20), η_1 and η_2 via (21) or (22), R_2 , R_1 and R_0 via (24), α and ϕ via (26), Δ via (25) and finally f via (27).

The system of linear equations that relates A_x , A_s and A_r is homogeneous, so the following amplitude ratios can be obtained:

$$\begin{aligned} \frac{A_x}{A_r} &= \frac{\xi \nu \eta_2 + \frac{1}{2}(1+\nu) \xi n \eta_2 \left[\eta_1 - \Delta \eta_1 + \frac{h^2}{12a^2} (\xi^4 \eta_1 + n^4 \eta_1 + 2\xi^2 n^2 \eta_2) \right]}{\frac{1}{2}(1+\nu) \xi^2 \nu n \eta_2^2 - n \eta_1 \left[\xi^2 \eta_1 + \frac{1}{2}(1-\nu) n^2 \eta_2 - \Delta \eta_2 \right]}, \\ \frac{A_s}{A_r} &= \frac{\left[\eta_1 - \Delta \eta_1 + \frac{h^2}{12a^2} (\xi^4 \eta_1 + n^4 \eta_1 + 2\xi^2 n^2 \eta_2) \right] \left[\xi^2 \eta_1 + \frac{1}{2}(1-\nu) n^2 \eta_2 - \Delta \eta_2 \right] - \xi^2 \nu^2 \eta_2}{\frac{1}{2}(1+\nu) \xi^2 \nu n \eta_2^2 - n \eta_1 \left[\xi^2 \eta_1 + \frac{1}{2}(1-\nu) n^2 \eta_2 - \Delta \eta_2 \right]} \end{aligned} \tag{28}$$

Therefore, for each mode shape (defined by a pair of values n and m), the model analytically provides three natural frequencies and two amplitude ratios. These results are in close correspondence with analogous studies [6,10,29]. Each vibration mode is characterized by one natural frequency and one mode shape. The essential difference between a vibration mode and another with the same mode shape consists, in addition to the frequency, in the

Table 1

Natural frequencies for $n \leq 14$ and $m \leq 10$ ($a=3$ in ≈ 76 mm, $l=12$ in ≈ 305 mm, $h=0.01$ in ≈ 0.254 mm, $\rho=0.283$ lb/in³ ≈ 7833 kg/m³, $E=30 \cdot 10^6$ psi ≈ 207 kN/mm², $\nu=0.3$).

n	m=1			m=2			m=3			m=4			m=5		
	f ₁ [Hz]	f ₂ [Hz]	f ₃ [Hz]	f ₁ [Hz]	f ₂ [Hz]	f ₃ [Hz]	f ₁ [Hz]	f ₂ [Hz]	f ₃ [Hz]	f ₁ [Hz]	f ₂ [Hz]	f ₃ [Hz]	f ₁ [Hz]	f ₂ [Hz]	f ₃ [Hz]
1	3653	15,226	20,208	6379	16,971	27,385	7904	20,213	35,633	8639	24,379	44,108	9000	29,006	52,703
2	2017	20,412	27,304	4033	22,467	32,715	5669	25,216	39,817	6834	28,565	47,587	7612	32,456	55,689
3	1192	25,505	36,998	2614	27,774	40,837	4011	30,542	46,465	5205	33,558	53,183	6150	36,961	60,524
4	772	31,052	47,458	1776	33,186	50,375	2892	35,911	54,829	3960	38,791	60,478	4901	41,926	66,945
5	564	36,938	58,227	1274	38,851	60,574	2146	41,416	64,206	3052	44,165	68,966	3914	47,122	74,604
6	501	43,041	69,155	980	44,741	71,116	1651	47,102	74,168	2400	49,691	78,238	3157	52,489	83,166
7	548	49,284	80,173	839	50,800	81,858	1335	52,959	84,485	1940	55,373	88,023	2587	58,011	92,366
8	668	55,622	91,249	823	56,984	92,725	1162	58,956	95,030	1631	61,199	98,151	2169	63,678	102,018
9	833	62,026	102,363	906	63,258	103,676	1113	65,066	105,729	1454	67,149	108,518	1883	69,473	111,994
10	1029	68,477	113,505	1058	69,601	114,687	1170	71,265	116,537	1395	73,201	119,056	1717	75,381	122,209
11	1252	74,965	124,666	1256	75,997	125,742	1308	77,535	127,424	1442	79,339	129,721	1665	81,384	132,603
12	1498	81,479	135,843	1489	82,433	136,829	1504	83,861	138,372	1574	85,547	140,481	1714	87,470	143,134
13	1767	88,015	147,030	1750	88,900	147,941	1743	90,232	149,366	1771	91,812	151,315	1849	93,624	153,772
14	2058	94,567	158,227	2037	95,393	159,073	2016	96,641	160,396	2017	98,126	162,209	2052	99,836	164,495
n	m=6			m=7			m=8			m=9			m=10		
	f ₁ [Hz]	f ₂ [Hz]	f ₃ [Hz]	f ₁ [Hz]	f ₂ [Hz]	f ₃ [Hz]	f ₁ [Hz]	f ₂ [Hz]	f ₃ [Hz]	f ₁ [Hz]	f ₂ [Hz]	f ₃ [Hz]	f ₁ [Hz]	f ₂ [Hz]	f ₃ [Hz]
1	9193	33,859	61,365	9305	38,834	70,069	9375	43,880	78,802	9423	48,971	87,555	9459	54,092	96,322
2	8127	36,731	63,985	8474	41,266	72,404	8715	45,975	80,908	8888	50,803	89,473	9018	55,716	98,084
3	6871	40,734	68,245	7413	44,812	76,214	7822	49,127	84,354	8135	53,623	92,620	8378	58,256	100,979
4	5693	45,354	73,965	6341	49,064	81,366	6866	53,022	89,040	7289	57,190	96,916	7632	61,527	104,944
5	4692	50,314	80,900	5371	53,749	87,683	5952	57,417	94,830	6445	61,295	102,255	6861	65,357	109,894
6	3878	55,497	88,788	4541	58,719	94,961	5134	62,153	101,566	5658	65,787	108,511	6117	69,605	115,729
7	3233	60,855	97,399	3852	63,898	103,006	4429	67,137	109,087	4955	70,565	115,554	5431	74,171	122,338
8	2733	66,364	106,547	3295	69,246	111,651	3836	72,315	117,245	4345	75,564	123,564	4818	78,985	129,613
9	2360	72,010	116,097	2856	74,741	120,761	3349	77,655	125,916	3828	80,744	131,499	4284	84,000	137,451
10	2104	77,775	125,952	2527	80,364	130,232	2965	83,135	134,995	3402	86,078	140,189	3830	89,183	145,762
11	1960	83,645	136,038	2305	86,100	139,986	2680	88,737	144,403	3068	91,543	149,245	3458	94,510	154,468
12	1923	89,606	146,305	2189	91,936	149,964	2495	94,446	154,074	2826	97,125	158,600	3171	99,963	163,504
13	1984	95,645	156,716	2174	97,858	160,121	2409	100,251	163,960	2679	102,810	168,202	2972	105,526	172,816
14	2129	101,751	167,240	2253	103,856	170,423	2421	106,138	174,021	2628	108,585	178,008	2864	111,188	182,359

relative amplitude of the displacements u_x , u_r and u_s , as showed in the following section.

Table 2
Amplitude ratios for $m \leq 10$ and $n=6$ ($a=3$ in ≈ 76 mm, $l=12$ in ≈ 305 mm, $h=0.01$ in ≈ 0.254 mm, $\rho=0.283$ lb/in $^3 \approx 7833$ kg/m 3 , $E=30 \cdot 10^6$ psi ≈ 207 kN/mm 2 , $\nu=0.3$).

	m=1		m=2		m=3		m=4		m=5	
	A_x/A_r	A_s/A_r								
f_1	0.06	0.17	0.07	0.17	0.09	0.17	0.08	0.18	0.09	0.16
f_2	29.00	3.28	13.68	3.43	9.46	3.86	7.69	4.21	6.66	4.77
f_3	1.24	6.09	2.19	6.33	3.32	6.70	4.68	7.19	6.23	7.74
	m=6		m=7		m=8		m=9		m=10	
	A_x/A_r	A_s/A_r								
f_1	0.07	0.18	0.08	0.15	0.06	0.17	0.07	0.13	0.05	0.15
f_2	6.17	5.27	5.86	5.99	5.78	6.67	5.74	7.56	5.84	8.44
f_3	8.03	8.38	9.98	8.99	12.16	9.69	14.44	10.28	16.90	10.95

4. Results and discussion

Table 1 shows the frequencies f_1 , f_2 and f_3 for a cylinder having the same geometric, physical and mechanical characteristics of those used by other authors [7,8,12]. It is interesting to note that the f_1 frequencies are smaller, by one or two orders of magnitude, than frequencies f_2 and f_3 . These results are in keeping with previous studies [7,8,12]. Furthermore, f_2 and f_3 increase monotonically with an increase in the number of n and m , which is in line with the results from the free vibrations of beams and plates, where the natural frequencies increase with the complexity of the waveforms. On the contrary, for fixed m and variable n , the f_1 frequencies show a minimum. The value of n for which f_1 is minimum grows as m increases. Additionally, at fixed n , the f_1 frequencies increase monotonically with m if $n < 12$, while showing a minimum for $n \geq 12$. The seemingly anomalous trend of the f_1 frequencies, which first decrease and then increase with n , was first observed by Arnold and Warburton [6] who, in the case of freely supported ends, were able to explain the phenomenon

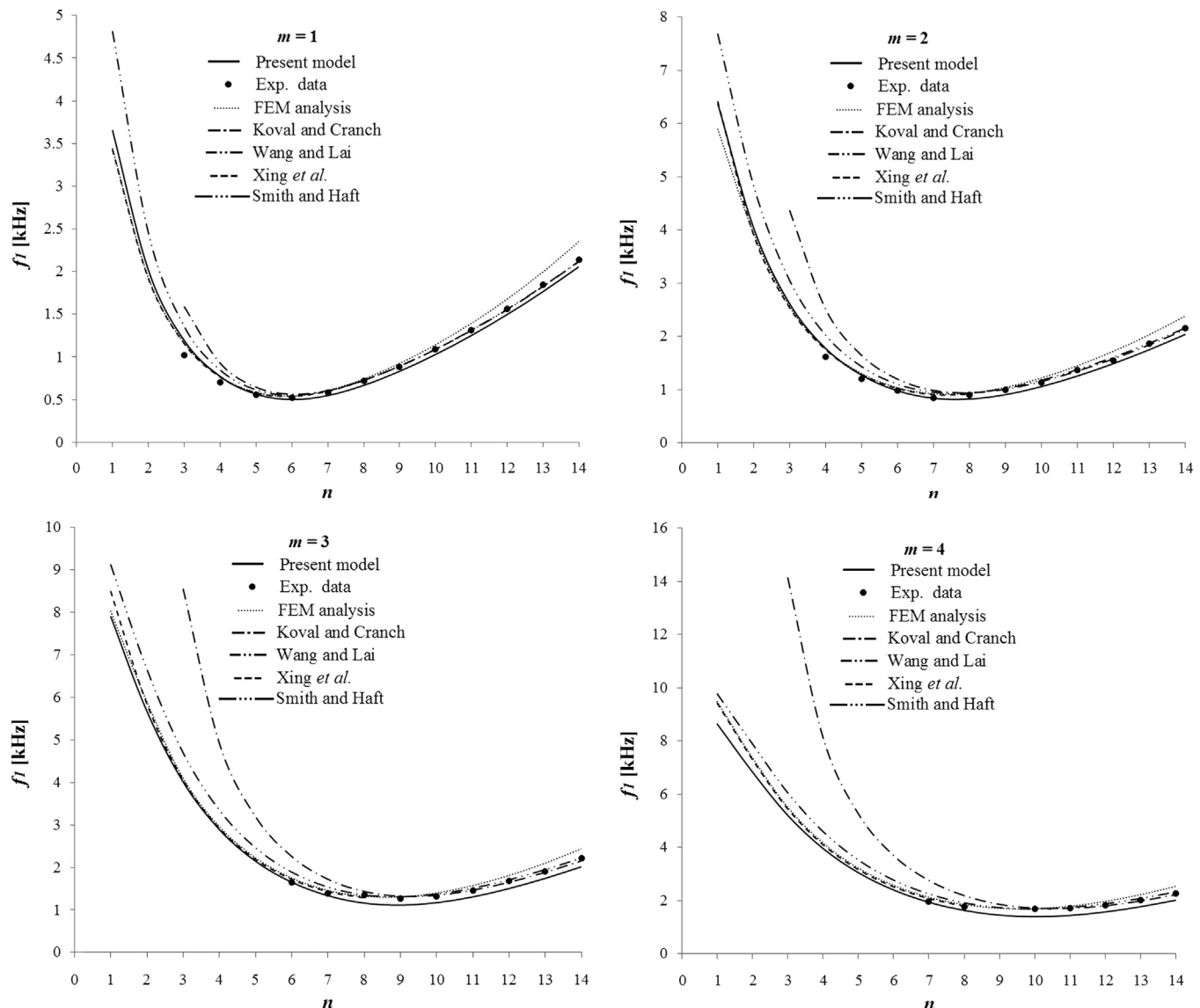


Fig. 5. Comparison between the f_1 natural frequencies calculated with the present model and other results, for $m \leq 4$ and $n \leq 14$ ($a=3$ in ≈ 76 mm, $l=12$ in ≈ 305 mm, $h=0.01$ in ≈ 0.254 mm, $\rho=0.283$ lb/in $^3 \approx 7833$ kg/m 3 , $E=30 \cdot 10^6$ psi ≈ 207 kN/mm 2 , $\nu=0.3$).

by considering the strain energy associated with bending and stretching of the reference surface.

Table 2 shows an example of the amplitude ratios (28) calculated for $m \leq 10$ and for $n=6$. Similar trends are obtained for other values of n . These results indicate that, at the lowest natural f_1 frequency, the predominant amplitude is A_r and the motion associated with this frequency is, therefore, mostly radial. This mode of free vibration is then called transverse mode. Conversely, at frequencies f_2 and f_3 , longitudinal motion and the circumferential motion, respectively, prevail for low values of m , while as m increases, the two components of motion assume similar amplitudes. Nevertheless, the mode of free vibration associated with f_2 is usually referred to as longitudinal mode and that associated with f_3 is called circumferential mode.

In the literature [6–13], particular attention was devoted to the study of the f_1 frequencies because of their greater importance to the resonance problems.

To check the validity of the model presented in this study, the calculated f_1 frequencies have been compared as a first step with the results of FEM modal analysis conducted by the authors. The FEM analysis was realized in ANSYS 14 using 5856 SHELL181 linear elements. This level of discretization was chosen after a convergence analysis that allowed the authors to assess the modal analysis results when decreasing the average size of the element. Successively, the model was validated against experimental data of Koval and Cranch [7] and versus results of other four models of literature: two numerical, i.e. Xing et al. [12] and Smith and Haft [8], and two analytical, i.e. Koval and Cranch [7] and Wang and Lai [10]. Fig. 5 shows these comparisons for the cases $m \leq 4$ and $n \leq 14$. As regards the Wang and Lai model, data were calculated

by the authors of the current work because those reported in [10] referred to a cylinder with different geometric and mechanical characteristics.

At a first glance, it is evident that the present model, the FEM analysis and the two numerical models are in good agreement both between themselves and with the experimental data, for all the investigated mode shapes; moreover the trends of the two numerical methods seem indistinguishable from one another. On the contrary the two analytical models part from other trends and become inaccurate for small values of n , as the same authors of the two models admit.

In light of the above, in the next steps, in order to quantify the percentage differences between the various results but also to reduce the number of possible comparisons only the most relevant results were taken into account, i.e. the mode shapes with $n \leq 8$. Moreover only the Wang and Lai analytical model and the Xing et al. numerical model were considered. The first, in effect, proved to be more accurate than Koval and Cranch model, while the second has been chosen since it uses the same indefinite equations of motion of the present paper but, using numerical methods of resolution, gets the “exact” solutions. This inducted the authors to consider these latter results, together with the experimental data of Koval and Cranch, as benchmark for assessing the accuracy of the present model. Tables 3 and 4 report these further outcomes. They show that the maximum error of the present model respect to the experimental data is less than 17% (for $m=1, n=3$) while the discrepancy respect to Xing et al. exact solutions is within a maximum of 10% (for $m=3, n=8$). However, it is worth noting that the maximum difference between the Xing et al. exact solutions and the experimental data is at 13% (for $m=1, n=3$). On the other

Table 3

Comparison of f_1 frequencies [Hz] from present model with other alternative studies for $m \leq 4$ and $n \leq 8$, ($a=3$ in ≈ 76 mm, $l=12$ in ≈ 305 mm, $h=0.01$ in ≈ 0.254 mm, $\rho=0.283$ lb/in³ ≈ 7833 kg/m³, $E=30 \cdot 10^6$ psi ≈ 207 kN/mm², $\nu=0.3$), n.a.=not available.

m	Method		n							
			1	2	3	4	5	6	7	8
1	Analytical	Present work	3653	2017	1192	772	564	501	548	668
		Koval and Cranch	n.a.	n.a.	1587	926	646	563	606	727
		Wang and Lai	4811	2452	1356	847	615	552	605	728
	Numerical	Xing et al.	3425	1917	1154	764	580	538	598	723
		Smith	3427	1918	1145	765	580	538	597	721
	FEM	Present work	3439	1928	1163	770	584	542	607	743
	Experimental	Koval and Cranch	n.a.	n.a.	1025	700	559	525	587	720
2	Analytical	Present work	6379	4033	2614	1776	1274	980	839	823
		Koval and Cranch	n.a.	n.a.	4365	2515	1645	1197	987	940
		Wang and Lai	7683	4824	3050	2025	1434	1103	953	939
	Numerical	Xing et al.	6412	3903	2537	1752	1287	1022	907	911
		Smith	6423	3905	2538	1753	1287	1022	907	911
	FEM	Present work	5893	3932	2560	1772	1304	1037	924	935
	Experimental	Koval and Cranch	n.a.	n.a.	n.a.	1620	1210	980	838	900
3	Analytical	Present work	7904	5669	4011	2892	2146	1651	1335	1162
		Koval and Cranch	n.a.	n.a.	8551	4921	3193	2256	1721	1434
		Wang and Lai	9120	6656	4695	3348	2461	1889	1538	1355
	Numerical	Xing et al.	8493	5841	4052	2920	2191	1720	1431	1287
		Smith	n.a.	5844	4054	2921	2192	1720	1431	1287
	FEM	Present work	8026	5893	4097	2959	2227	1752	1462	1321
	Experimental	Koval and Cranch	n.a.	n.a.	n.a.	n.a.	n.a.	1650	1395	1350
4	Analytical	Present work	8639	6834	5205	3960	3052	2400	1940	1631
		Koval and Cranch	n.a.	n.a.	14,135	8133	5267	3695	2759	2190
		Wang and Lai	9774	7889	6053	4597	3529	2771	2251	1917
	Numerical	Xing et al.	9420	7299	5444	4102	3167	2518	2077	1797
		Smith	n.a.	7303	5447	4104	3168	2516	2076	1797
	FEM	Present work	9479	7370	5512	4166	3227	2574	2130	1850
	Experimental	Koval and Cranch	n.a.	n.a.	n.a.	n.a.	n.a.	n.a.	1960	1765

Table 4
Comparison of the percentage errors on the f_1 frequencies for $m \leq 4$ and $n \leq 8$, ($a=3$ in ≈ 76 mm, $l=12$ in ≈ 305 mm, $h=0.01$ in $=0.254$ mm, $\rho=0.283$ lb/in³ ≈ 7833 kg/m³, $E=30 \cdot 10^6$ psi ≈ 207 kN/mm², $\nu=0.3$), n.a.=not available.

m	Comparison	n							
		1	2	3	4	5	6	7	8
1	Present vs experimental	n.a.	n.a.	16.3%	10.2%	0.9%	-4.6%	-6.6%	-7.2%
	Present vs Xing et al.	6.7%	5.2%	3.3%	1.0%	-2.8%	-6.9%	-8.3%	-7.6%
	Wang and Lai vs experimental	n.a.	n.a.	32.3%	20.9%	10.0%	5.2%	3.0%	1.0%
	Wang and Lai vs Xing et al.	40.5%	27.9%	17.5%	10.8%	6.0%	2.6%	1.1%	0.6%
	Xing et al. vs experimental	n.a.	n.a.	12.6%	9.1%	3.8%	2.5%	1.9%	0.4%
2	Present vs experimental	n.a.	n.a.	n.a.	9.6%	5.3%	0.0%	0.1%	-8.5%
	Present vs Xing et al.	-0.5%	3.3%	3.0%	1.4%	-1.0%	-4.1%	-7.5%	-9.6%
	Wang and Lai vs experimental	n.a.	n.a.	n.a.	25.0%	18.5%	12.6%	13.7%	4.3%
	Wang and Lai vs Xing et al.	19.8%	23.6%	20.2%	15.6%	11.4%	8.0%	5.0%	3.0%
	Xing et al. vs experimental	n.a.	n.a.	n.a.	8.1%	6.4%	4.3%	8.2%	1.2%
3	Present vs experimental	n.a.	n.a.	n.a.	n.a.	n.a.	0.1%	-4.3%	-14.0%
	Present vs Xing et al.	-6.9%	-2.9%	-1.0%	-1.0%	-2.0%	-4.0%	-6.7%	-9.7%
	Wang and Lai vs experimental	n.a.	n.a.	n.a.	n.a.	n.a.	14.5%	10.2%	0.4%
	Wang and Lai vs Xing et al.	7.4%	14.0%	15.9%	14.6%	12.3%	9.8%	7.4%	5.3%
	Xing et al. vs experimental	n.a.	n.a.	n.a.	n.a.	n.a.	4.2%	2.6%	-4.7%
4	Present vs experimental	n.a.	n.a.	n.a.	n.a.	n.a.	n.a.	-1.0%	-7.6%
	Present vs Xing et al.	-8.3%	-6.4%	-4.4%	-3.5%	-3.6%	-4.7%	-6.6%	-9.2%
	Wang and Lai vs experimental	n.a.	n.a.	n.a.	n.a.	n.a.	n.a.	14.9%	8.6%
	Wang and Lai vs Xing et al.	3.8%	8.1%	11.2%	12.1%	11.4%	10.1%	8.4%	6.7%
	Xing et al. vs experimental	n.a.	n.a.	n.a.	n.a.	n.a.	n.a.	6.0%	1.8%

hand, it is also to be considered that the disagreement between theory and experiments could be partly due to the imperfect clamping of the experimental specimens as well as to the unavoidable measurement error.

As regards the Wang and Lai analytical model, the maximum error is at 33% (for $m=1$, $n=3$) respect to the experimental data and at 41% (for $m=1$, $n=1$) versus Xing *et al.*

Finally, with reference to the lowest experimental natural frequency, properly identified by all models for $m=1$ and $n=6$, the present model gives an underestimation of 4.6%, Xing *et al.* an overestimation of 2.5% and Wang and Lai an overestimation of 5.2%.

From the analysis of the above results, it can be concluded that the presented model is only a bit less accurate of the exact solutions found numerically, also for those mode shapes for which the other analytical models, more or less, fail. Moreover the present model is the only one that has slightly underestimated the lowest natural frequency and this could result in the advantage of safely identifying the first resonance frequency of the real physical system. Lastly, the lower accuracy of the present model respect to the numerical ones, is widely compensated by its much greater ease of use and by its low computational cost, without iterative calculations and without problems of convergence of the solution.

5. Conclusion

In this paper, a new mathematical model to calculate the natural frequencies of isotropic thin-walled circular cylindrical shells with clamped edges was presented.

The joint use of Hamilton's principle and of a solving technique similar to Rayleigh's method, as well as of a proper methodology for the derivation of the eigenfunctions, allows for an explicit closed-form solution that combines good precision with ease of calculation: given the geometric and mechanical

characteristics of the cylinder, it carefully provides the natural frequencies via a sequence of explicit algebraic equations. Other models present in the literature obtain a little higher accuracy but via numerical resolutions of the differential equations of motion, with the related complexity of implementation and of solution convergence. Other analytical models have ease of calculation comparable to the present model but fail for a small value of circumferential waves.

A comparative analysis with experimental and numerical data from the literature showed that the maximum error respect to the exact solutions is less than 10% for all the comparable mode shapes and less than 5%, on the safe side, respect to the experimental data for the lowest natural frequency.

Therefore the advantage of this novel model respect to the others consists in a best balance between simplicity and accuracy resulting an ideal tool for engineers who design such shells structures.

Extensions of the present approach for different boundary conditions and for the case of rotating shells are under consideration. The real constraints are yielding, and the use of proper suspension systems could have a beneficial effect on rotor hysteretic instability [30,31]. Furthermore, when shells of revolutions rotate, it is necessary to take into account the Coriolis and centrifugal accelerations as well as the hoop tension due to angular velocities in the differential equations of motion. These effects have significant influence on the dynamic behaviour of rotating shells, and their structural frequency characteristics are qualitatively altered [32–34].

Acknowledgement

This research is part of the DIT (Dynamics Irreversible Thermoporation) project supported by the European Union's PO FESR 2007/2013 fund.

Appendix

In general, the displacement of a point in a thin shell is a function of the position and of the time, i.e.

$$u = u(x, \theta, t)$$

however, in order to find approximate solutions of the indefinite equations of motion, analogously to other problems regarding vibrations of continuous systems, it is convenient to write each eigenfunction in the form

$$u_{...} = A_{...} \cdot f_{...}(x) \cdot g_{...}(\theta) \cdot \cos \omega t$$

The clamped-clamped boundary conditions require (see Eqs. (8) and (2.2)):

$$\begin{cases} u_x = u_s = u_r = 0 \\ \frac{\partial u_r}{\partial x} = \frac{\partial u_r}{\partial \theta} = 0 \end{cases} \text{ for } x = 0 \text{ and } x = 1 \quad (\text{A.1})$$

while the mutual orthogonality conditions require:

$$\begin{cases} \int_V u_r u_x dV = 0 \\ \int_V u_r u_s dV = 0 \end{cases}$$

where V is the volume of the cylinder, and so

$$\begin{cases} \int_0^l f_r(x) f_x(x) dx \int_0^{2\pi} g_r(\theta) g_x(\theta) d\theta = 0 \\ \int_0^l f_r(x) f_s(x) dx \int_0^{2\pi} g_r(\theta) g_s(\theta) d\theta = 0 \end{cases} \quad (\text{A.2})$$

Considering that the shape of the circumferential waves is independent of the boundary conditions while the shape of the longitudinal half-waves depends on boundary conditions and is similar to the flexural vibrations of $g_r(\theta) = \cos(n\theta)$ beams subject to the same constraints [10,13], for the radial displacement u_r , it is suitable to choose $f_r(x)$ similar to the eigenfunctions of the beam subject to the same constraints. As regards the functions $g_{...}(\theta)$ and $f_{...}(x)$ of the other displacements, u_x and u_s , it is easy to see that both the boundary conditions and the mutual orthogonality conditions result identically satisfied if one puts

$$f_x(x) \propto \frac{d}{dx} f_r(x)$$

$$g_x(\theta) \propto g_r(\theta)$$

$$f_s(x) \propto f_r(x)$$

$$g_s(\theta) \propto \frac{d}{d\theta} g_r(\theta)$$

and therefore:

$$\begin{cases} u_x = A_x \cdot \frac{d}{dx} f_r(x) \cdot \cos(n\theta) \cdot \cos \omega t \\ u_s = A_s \cdot f_r(x) \cdot \sin(n\theta) \cdot \cos \omega t \\ u_r = A_r \cdot f_r(x) \cdot \cos(n\theta) \cdot \cos \omega t \end{cases} \quad (\text{A.3})$$

$$\begin{cases} \frac{\partial u_r}{\partial x} = A_r \cdot \frac{d}{dx} f_r(x) \cdot \cos(n\theta) \cdot \cos \omega t \\ \frac{\partial u_r}{\partial \theta} = -n \cdot A_r \cdot f_r(x) \cdot \sin(n\theta) \cdot \cos \omega t \end{cases} \quad (\text{A.4})$$

In this way, all the functions (A.3) and (A.4) are proportional to f_r or to $\frac{df_r}{dx}$ and, being f_r the eigenfunction of the clamped-clamped beam, $f_r = 0$ and $\frac{df_r}{dx} = 0$ at either end, and consequently the boundary conditions (A.1) result satisfied.

Moreover, the mutual orthogonality conditions (A.2) reduce to

$$\begin{cases} \int_0^l f_r^{(l)} f_r df_r \int_0^{2\pi} [g_r(\theta)]^2 d\theta = 0 \\ \int_0^l [f_r(x)]^2 dx \int_0^{2\pi} g_r dg_r = 0 \end{cases} \quad (\text{A.5})$$

which are identically satisfied because the upper and the lower

integration limits in the first or in the second integral of Eq. (A.5) are equal (remember that $g_r(\theta) = \cos(n\theta)$).

As regards the most convenient form to be given to the $f_r(x)$ function, consider the following.

As well known, the mode shapes of the clamped-clamped beam are proportional to:

$$f_r(x) = (\sin \mu X - \sinh \mu X) + \Psi (\cos \mu X - \cosh \mu X)$$

where $X = x/l$, $\Psi = \frac{\sinh \mu - \sin \mu}{\cos \mu - \cosh \mu}$ and μ indicates one of the infinite roots of the frequency equation $\cos \mu \cosh \mu = 1$.

Therefore, substituting into Eq. (10) both the partial derivatives $\partial_{...}$ and the virtual displacements $\delta_{...}$ of u_x , u_s and u_r , we will have 80 addends in the first line, 80 in the second, and 112 in the third, for a total of 272 initial addends to be collected and then integrated. However, the symmetry of the boundary conditions may yield a simplified expression for $f_r(x)$ with only two addends provided that the symmetric and anti-symmetric waves are considered separately. In this way, we have 20 addends in the first line, 20 in the second, and 28 in the third, for a total of 68 initial addends to be collected and integrated.

Then, for the odd numbers m of the longitudinal half-waves, the eigenfunctions can be written as:

$$f_r(x) = \cos \mu \left(\frac{1}{2} - X \right) + \Psi \cosh \mu \left(\frac{1}{2} - X \right) \quad (\text{A.6})$$

where to comply with the boundary conditions $\Psi = \frac{\sin(\mu/2)}{\sinh(\mu/2)}$ and μ must satisfy the equation

$$\tan \frac{\mu}{2} + \tanh \frac{\mu}{2} = 0, \text{ whose roots are } \mu \approx [1.506 + (m-1)\pi].$$

For the even numbers m of the longitudinal half-waves Eq. (A.6) must be modified by replacing $\cos \leftarrow \sin$, $\cosh \leftarrow -\sinh$, so

$$f_r(x) = \sin \mu \left(\frac{1}{2} - X \right) - \Psi \sinh \mu \left(\frac{1}{2} - X \right) \quad (\text{A.7})$$

in which ψ is the same as before but μ , this time, must satisfy the equation $\tan \frac{\mu}{2} - \tanh \frac{\mu}{2} = 0$, whose roots are $\mu \approx [2.500 + (m-2)\pi]$.

Therefore, finally, replacing Eqs. (A.6) or (A.7) into Eq. (A.3) one gets Eqs. (11) and (15) respectively.

References

- [1] Love AEH. The small free vibration and deformation of thin elastic shells. Philos Trans R Soc Lond 1888;179A:491–546.
- [2] Leissa AW. Vibration of shells, NASA SP288. Washington DC: US Government Printing Office; 1973.
- [3] Qatu MS. Recent research advances in the dynamic behavior of shells:1989–2000, part 2: homogeneous shells. ASME Appl Mech Rev 2002;55:415–34.
- [4] Qatu MS, Sullivan RW, Wang W. Recent research advances on the dynamic analysis of composite shells: 2000–2009. Compos Struct 2010;93:14–31.
- [5] Kiran Kumar P, Subrahmanyam JV, Ramalakshmi P. A review on non linear vibration of thin shells. Int J Eng Res Appl 2013;3:181–207.
- [6] Arnold RN, Warburton GB. Flexural vibration of the walls of thin cylindrical shells having freely supported ends. Proc R Soc Lond 1949;197A:238–56.
- [7] Koval LR, Cranch ET. On the free vibration of thin cylindrical shells subjected to an initial static torque. In: Proceedings of the 4th U.S. national congress of applied mechanics; 1962. p.107–17.
- [8] Smith BL, Haft EE. Natural frequencies of clamped cylindrical shells. AIAA J 1967;6:720–1.
- [9] Callahan J, Baruh H. A closed-form solution procedure for circular cylindrical shell vibrations. Int J Solid Struct 1999;36:2973–3013.
- [10] Wang C, Lai JCS. Prediction of natural frequencies of finite length circular cylindrical shells. Appl Acoust 2000;59:385–400.
- [11] Pellicano F. Vibrations of circular cylindrical shells: theory and experiments. J Sound Vib 2007;303:154–70.
- [12] Xing Y, Liu B, Xu T. Exact solutions for free vibration of circular cylindrical shells with classical boundary conditions. Int J Mech Sci 2013;75:178–88.
- [13] Xie X, Jin G, e Liu Z. Free vibration analysis of cylindrical shells using the Haar wavelet method. Int J Mech Sci 2013;77:47–56.
- [14] Silvestre N, Wang CM, Zhang YY, Xiang Y. Sanders shell model for buckling of single-walled carbon nanotubes with small aspect ratio. Compos Struct 2011;93:1683–91.

- [15] Timoshenko S. *Theory of plates and shells*. 1st ed.. New York: McGraw-hill; 1940.
- [16] Donnell LH. *Stability of thin walled tubes under torsion*. United States: National Advisory Committee on Aeronautics; 1933 Report no.479.
- [17] Flügge W. *Stresses in shells*. Berlin: Springer-Verlag; 1962.
- [18] Yu YY. Free vibration of thin cylindrical shells having finite lengths with freely supported and clamped edges. *J Appl Mech* 1955;77:547–52.
- [19] Xuebin L. A new approach for free vibration analysis of thin circular cylindrical shell. *J Sound Vib* 2006;296:91–8.
- [20] Chung H. Free vibration analysis of circular cylindrical shells. *J Sound Vib* 1981;74(3):331–50.
- [21] Junger MC, D. Feit. *Structures and their interaction*. Cambridge: MIT Press; 1972.
- [22] Sanders JLR. Nonlinear theories for thin shells. *Q Appl Math* 1963;21:21–36.
- [23] Koiter WT. On the nonlinear theory of thin elastic shells. In: *Proceedings koninklijke nederlandse akademie van wetenschappen*; 1966. Vol. 69B. p. 1–54.
- [24] Mushtari KHM. On the stability of cylindrical shells subjected to torsion. Russia: Kazan Aviatcionnugo Inatituta; 1938. p. 2.
- [25] Zhang L, Xiang Y, Wei GW. Local adaptive differential quadrature for free vibration analysis of cylindrical shells with various boundary conditions. *Int J Mech Sci* 2006;48:1126–38.
- [26] Goldenvejzer AL, Lidskij VB, Tovstik PE. *Free vibrations of thin elastic shells*. Moscow: Nauka; 1979.
- [27] Khalili SMR, Davar A, Malekzadeh Fard K. Free vibration analysis of homogeneous isotropic circular cylindrical shells based on a new three-dimensional refined higher-order theory. *Int J Mech Sci* 2012;56:1–25.
- [28] Reissner E. A new derivation of the equations for the deformation of elastic shells. *Am J Math* 1941;63:177–84.
- [29] Miller PR. *Free vibration of a stiffened cylindrical shell*. Aeronautical Research Council Reports and Memoranda no. 3154. London; 1960.
- [30] Sorge F, Cammalleri M. Control of hysteretic instability in rotating machinery by elastic suspension systems subject to dry and viscous friction. *J Sound Vib* 2010;329:1686–701.
- [31] Sorge F, Cammalleri M. On the beneficial effect of rotor suspension anisotropy on viscous-dry hysteretic instability. *Meccanica* 2012;47:1705–22. <http://dx.doi.org/10.1007/s11012-012-9549-y>.
- [32] Li H, Lam KY, Ng TY. *Rotating shell dynamics*. 1st ed.. London: Elsevier; 2005.
- [33] Chen Y, Zhao HB, Shen ZP, Grieger I, Kröplin BH. Vibration of high speed rotating shells with calculations for cylindrical shells. *J Sound Vib* 1993;160(1):137–60.
- [34] Li H, Lam KY. Frequency characteristics of a thin rotating cylindrical shell using the generalized differential quadrature method. *Int J Mech Sci* 1998;40:443–59.